

Design of a circular clamped plate excited by a voice coil and piezoelectric patches used as a loudspeaker

Olivier Doaré*

ENSTA-Paristech, UME,
Boulevard des Maréchaux,
91762, Palaiseau Cedex, France

Gérald Kergourlay

Canon Research Centre France S.A.S,
Rue de la Touche-Lambert,
35510, Cesson Sevigne, France

Clément Sambuc

ENSTA-Paristech, UME,
Boulevard des Maréchaux,
91762, Palaiseau Cedex, France

In this article a dynamical model of the vibrations and acoustic radiation of a circular clamped plate excited by a voice coil and two annular piezoelectric patches is derived. This model is used to perform an optimization of the geometries with the objective to minimize the vibration of the plate along its second and third modes, so that the plate's radiation is equilibrated between its first and fourth eigenfrequencies. Experiments are then performed and show a good agreement with the model. Radiation of the designed system presents improvements when compared to a system when only a voice coil is used.

Nomenclature

W Plate's vertical displacement (m), non-dimensional $\rightsquigarrow w$
 R Radius variable (m), non-dimensional $\rightsquigarrow r$
 T Time (s), non-dimensional $\rightsquigarrow t$
 A, B Internal, external radii of piezo (m), non-dimensional $\rightsquigarrow a, b$
 C Radius of voice coil (m), non-dimensional $\rightsquigarrow c$
 R_0 Plate's radius, non-dimensional $\rightsquigarrow 1$
 E_0, E_p Young's modulus of plate and piezo
 ν_0, ν_p, ν_g Poissons's coefficient of plate, piezo and glue
 ρ_0, ρ_p, ρ_g Density of plate, piezo and glue
 H_0 Plate's thickness (m)
 H_p Piezos thickness (m)
 H_g Glue thickness (m)
 μ_0, μ_p, μ_g Surface density of plate, piezos and glue layer
 D_0 Rigidity of plate = $E_0/12(1 - \nu_0^2)$
 D_p Rigidity of piezos = $E_p/(1 - \nu_p^2) \times (H_p H_0^2/2 + H_p^2 H_0 + 2H_p^3/3)$
 M_0 Total mass of the plate (kg)
 R_c Electrical resistance of the voice coil (Ohms)

L_c Inductance of the voice coil (H)
 Bl Electromechanical conversion factor (T.m)
 u_c, u_p Tension across the voice coil and the piezo respectively (V)
 Z_p Moment arm of the piezoelectric patch $\equiv \left(\frac{H_0 + H_p}{2} \right)$

1 Introduction

Classically, sound is produced by exciting air with a moving surface. The manufacturing of loudspeakers has converged to a design involving a cone excited at a given radius by a voice coil and fixed at its outer radius to a rigid structure through a flexible material, referred to as the surround. As a first approach, the radiation behavior of such designed loudspeakers can be estimated by considering a translating plane surface baffled in an enclosure and coupled to an electrical circuit. This assumption served as a basis for the theory of Thiele [1, 2] in the context of closed boxes and Small [3, 4] for vented boxes. They are yet widely used for the design complete loudspeaker systems in the industry. In practice, such system possesses also structural modes at higher frequencies [5]. The useful bandwidth of this kind of loudspeakers (*i.e.* the frequency range where the radiated power is almost constant and suitable for high-fidelity reproduction) is in practice comprised between the two first eigenfrequencies of the system. Hence, with this design, the higher the first eigenfrequency of the structural modes compared to the frequency piston-like oscillator, the wider the bandwidth. That is one of the reasons why a conical membrane is used. One can find many attempts to depart from this now classical piston-like design. In addition to designs involving piezoelectric transducers [6], one can mention systems involving rectangular plates excited by multiple electrodynamic transducers, at the origin of the DML system [7, 8]. Other systems

*Corresponding author: olivier.doare@ensta-paristech.fr

involving rectangular panels are used to synthesize acoustical wave fields [9, 10], and thus referred to as Wave Field Synthesis.

The present article addresses the problem of a loudspeaker consisting of a circular plate clamped at its outer radius, excited by a voice coil. Attention is paid on this system because it makes possible the design of flat loudspeakers, and a deformation along its first mode presents a better directivity factor than a translating baffled piston mode [11]. This design has however a major inconvenience: compared to piston-like structures, the first eigenfrequency is poorly separated from the others. The bandwidth of such a transducer is hence significantly reduced in comparison to the classical design. In order to circumvent this problem, we treat the reduction of the vibrations of the undesirable modes with the introduction of additional forcings on the system exerted by piezoelectric patches. Vibrating plates or beams equipped with piezoelectric elements interacting with electric circuits have been extensively studied during the last decades, in various application fields such as active control of undesirable vibrations [12], aeroelastic instabilities [13, 14], passive damping [15–17], energy harvesting [18–21]. In the specific domain of acoustics, piezoelectric actuators and sensors have been used to control the sound radiated by vibrating plates [22–26], the sound transmitted by plates between two spaces [27–29]. Piezoelectric coupling will be introduced in the present work using results of Lee et al. [30, 31], who derived the equations governing the dynamics of a general non-isotropic three layered laminated plate with two symmetric piezoelectric layers.

The work of the present article has for objective to find the optimal geometric parameters of the voice coil and the piezoelectric patches so that the plate's response has a maximal amplitude along its first mode and a minimal amplitude at the other ones when the same signal is sent to all actuators. The paper is organized as follows. In section 2, a dynamical model of a flat circular clamped plate equipped with a voice coil and two piezoelectric patches is derived. In section 3, this model is used to perform an optimization with the objective above mentioned. In section 4, various experimental and theoretical transfer functions are compared to validate the model and results of a controlled loudspeaker are presented. A conclusion then closes the article.

2 Reduced order model of a plate equipped with a voice coil and two symmetrical piezoelectric annuli

2.1 Position of the problem

In this section, a reduced order dynamical model of a flat circular clamped plate equipped with a voice coil and two piezoelectric patches is presented. Firstly, dynamical equations of a plate with added mass and rigidity due to the presence of piezoelectric patches are derived. A modal expansion will then be performed and the full dynamical equations of the plate with piezoelectric patches, voice coil and their associated forcings will be projected on the eigenmodes to obtain a linear discrete dynamical system where each modal displacement and electrical displacements of each electrical

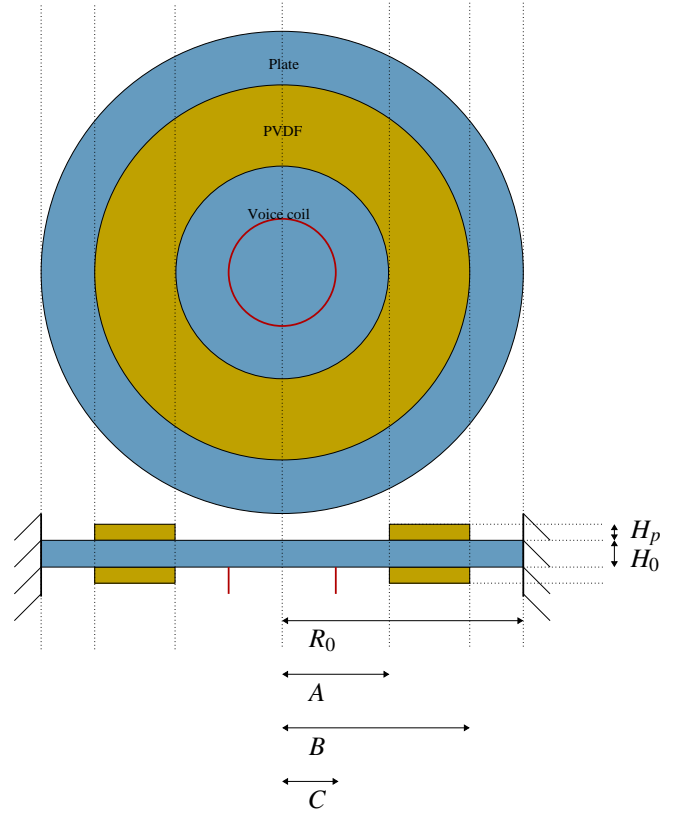


Fig. 1. Schematic view of a flat plate loudspeaker with a voice coil and two piezoelectric patches.

circuit represent one degree of freedom. This model will then be used to compute various electromechanical transfer functions.

2.2 Equations and eigenmodes of a plate with piezoelectric patches

Consider the system sketched in Figure 1, representing a plate of thickness H_0 , radius R_0 on which two piezoelectric annuli of internal radius A , external radius B and thickness H_p are glued. A voice coil of mass M_c is fixed at $R = C$ on the plate. Due to the presence of two piezoelectric layers between the radii A and B , the flexural rigidity of the plate has the following expression,

$$D(R) = D_0 + F_p(R)D_p, \quad (1)$$

where D_0 is the flexural rigidity of the plate without piezoelectric layers, D_p is an added flexural rigidity due to the presence of the piezoelectric material and F_p is a function that equals 1 for $R \in [A, B]$ and zero elsewhere, so that is it appropriately described by the sum of two Heaviside functions,

$$F_p(R) = H(R - A) - H(R - B). \quad (2)$$

The exact expression of the flexural rigidity D_p as function of the material properties and their geometries has been derived

in the case of a three layer laminate by Lee et al. [30–32] and is given in the nomenclature. We may also consider the five layer problem where two additional layers of glue are considered. It is presented in appendix B. It is shown in this appendix that it is possible to end up with an equivalent three layer problem after an appropriate change of variables. Thus the three layer model is retained here for the sake of simplicity.

The surface density of the plate has the following expression,

$$\mu(R) = \mu_0 + F_p(R)\mu_p + \delta(R - C)\frac{M_c}{2\pi C}, \quad (3)$$

where μ_0 and μ_p are the surface density of the plate and the two piezoelectric patches respectively. Using a linear Kirchoff-Love approximation, the displacement of the plate is known to satisfy the following equation:

$$D(R)\Delta^2 W(R, T) + \mu(R)\ddot{W}(R, T) = P(R, T). \quad (4)$$

where P is the pressure exerted on the plate. The plate's displacement is here considered independent of the polar angle, which is justified by the fact that all forcings exerted on the plate are axisymmetric. The boundary conditions of the problem are classical boundary conditions of a plate clamped at $R = R_0$,

$$W(R = R_0, T) = \left. \frac{\partial W(R, T)}{\partial T} \right|_{R=R_0} = 0. \quad (5)$$

Three kind of external forcing are now considered: the force coming from the voice coil P_c , the force due to piezoelectric coupling P_p , and a force due to a pressure difference between each side of the plate P_v .

Following the modelization of Thiele [1,2] of electromechanical coupling introduced in the context of piston-like electrodynamic transducers, the force exerted by the voice coil is considered to be proportional to the electrical current in the coil i_c , to the radial magnetic flux density in the air gap B and to the length of the wire in the magnetic field l . This force is then exerted on a circle of radius C so that its contribution in the right-hand term of equation (4) reads,

$$P_c(R, T) = Bl i_c(T) \frac{\delta(R - C)}{2\pi C}. \quad (6)$$

The pressure P_p is a consequence of the stretching of the piezoelectric material induced by charge displacements. Its expression can be deduced from the results of Lee and Moon [30], where it is expressed in cartesian coordinates in the general case of non-isotropic piezoelectric materials. Considering isotropy in the plane (X, Y) (*i.e.* the plane of the plate) and axisymetry, the contribution of one piezoelectric patch in the right-hand term of equation (4) is readily

obtained in polar coordinates as

$$P_p(R, T) = -u_p(T)e_{31}Z_p \left(\frac{\partial^2 F_p}{\partial R^2} + \frac{1}{R} \frac{\partial F_p}{\partial R} \right), \quad (7)$$

where u_p is the voltage at the outlets of the piezoelectric element, e_{31} is a piezoelectric coefficient describing the coupling between the deformation in the plane of the plate to the electrical field in the Z -direction. In the present approach, two symmetrically glued piezoelectric patches are considered, each are connected to a distinct circuit. In many works, piezoelectric patches are glued in such a way that their respective polarity is inverted. Connected in series, they behave like a single piezoelectric patch with a moment arm of twice the value in equation (7) and an electric capacity of two condensers in series, $C_p/2$. This configuration is in practice that which induces the smallest non-linear effects, not modeled in the present approach. Indeed, this configuration ensures that the longitudinal stretching of the plate induced by one piezoelectric patch is cancelled by the other [12]. In the present model, the voltages exerted on both piezoelectric elements are always equal, thus leading to the same conclusion, but it leaves the possibility to use non-symmetric forcings for which the present model is valid only at the linear level.

If the loudspeaker is placed in a closed box of volume V_0 at static equilibrium, there is a pressure difference between each side of the plate, due to the volume variation of the box. This pressure is hence expressed as

$$P_v = \delta P = -\gamma P_a \frac{\delta V}{V_0} = -\gamma P_a \frac{\int_S W(R, T) dS}{V_0}. \quad (8)$$

This expression is similar to those found in models considering piston-like loudspeaker [3, 4]. The difference comes from the fact that the plate's displacement depends on r in the present model and has to be integrated to compute the volume variation.

Let us now consider the electrical networks on which the electromechanical devices are connected. The electrical network considered for the voice coil is sketched in Figure 2a. It consists of a resistance R_c , an inductance L_c and a power source $BIW(T)$ due to the electromechanical coupling. A voltage source coming from an amplifier is connected in parallel of these three elements. The model equation of this electrical network is then,

$$R_c i_c(T) + L_c \frac{di_c}{dT} + Bl \frac{dW(C)}{dT} = u_c(t). \quad (9)$$

The equivalent electrical network for the piezoelectric patches is sketched in Figure 2b and is considered when the piezoelectric material is used as an actuator. Here a voltage signal u_p coming from an amplifier is connected directly to the outlets of the piezoelectric material, which behaves as a capacitive element in series with a power source due to

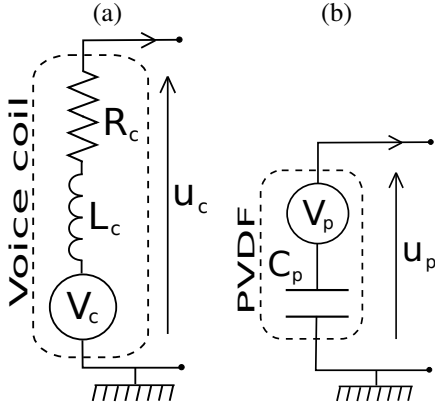


Fig. 2. Models of electrical circuits for the voice coil (a) and the piezoelectric patch (b).

the electromechanical coupling. The equation governing the electric charge displacement Q_p reads [30],

$$\frac{Q_p}{C_p} + \frac{Z_p e_{31}}{C_p} \int_S F_p(R) \left(\frac{\partial^2 W}{\partial R^2} + \frac{1}{R} \frac{\partial W}{\partial R} \right) dS = u_p(t). \quad (10)$$

Non-dimensional equations are now derived. Introducing the non-dimensional radius, displacement, time and pressure as

$$r = R/R_0, \quad w = W/H_0, \quad t = \frac{T}{T_c} = \frac{T}{R_0^2 \sqrt{\frac{\mu_0}{D_0}}}, \quad p = \frac{P}{\frac{D_0 H_0}{R_0^4}}, \quad (11)$$

the non-dimensional local equilibrium equation (4) becomes,

$$\bar{D}(r) \Delta^2 w + \bar{\mu}(r) \dot{w} = p(r, t), \quad (12)$$

with

$$\bar{D}(r) = 1 + \bar{D}_p f_p, \quad (13)$$

$$\bar{\mu}(r) = 1 + \bar{\mu}_p f_p + \frac{\delta(r-c)}{2c} \bar{M}_c \quad (14)$$

$$f_p(r) = H(r-a) - H(r-b), \quad (15)$$

and where $a = A/R_0$ and $b = B/R_0$ are the non-dimensional radii characterizing the piezoelectric annulus geometry, $\bar{D}_p = D_p/D_0$ is the non-dimensional flexural rigidity of the three-layers laminate, $\bar{\mu}_p = \mu_p/\mu_0$ is the non-dimensional surface density and $\bar{M}_c = M_c/M_0$ is the mass of the voice coil normalized by the mass of the plate. The dimensionless pressure due to external forcings on the plate is similarly decomposed into three components $p = p_c + p_p + p_v$ with,

$$p_c(r, t) = \bar{\tau}_c i_c(t) \frac{\delta(r-c)}{2\pi c}, \quad (16)$$

$$p_p(r, t) = -\bar{\tau}_p u_p(t) \left(\frac{\partial^2 f_p}{\partial r^2} + \frac{1}{r} \frac{\partial f_p}{\partial r} \right), \quad (17)$$

$$p_v(r, t) = -\bar{\tau}_v 2\pi \int_0^1 w(r, t) r dr, \quad (18)$$

where $q = q/T_c$, and where the three following coupling coefficients have been introduced:

$$\bar{\tau}_c = \frac{BIR_0^2}{D_0 H_0}, \quad (19)$$

$$\bar{\tau}_p = \frac{Z_p e_{31} R_0^2}{D_0 H_0}, \quad (20)$$

$$\bar{\tau}_v = \frac{\gamma P_a R_0^6}{V_0 D_0}. \quad (21)$$

The coefficient $\bar{\tau}_c$ quantifies the coupling between the current in the voice coil and the dimensionless force exerted on the plate. $\bar{\tau}_p$ quantifies the coupling between the current in the piezoelectric patches and the force exerted on the plate. Finally, $\bar{\tau}_v$ quantifies the force exerted on the plate due to a volume variation in the closed box. It has to be noted that q is not a dimensionless quantity as it has the dimensions of an electric charge per unit time. This normalization is preferred because it allows to keep voltages and currents expressed in Volts and Amperes respectively while all purely mechanical quantities are dimensionless. Another consequence is that q , \dot{q} and \ddot{q} have all the dimension of Amperes while $\bar{\tau}_c$ and $\bar{\tau}_p$ have the dimension of Amperes⁻¹. The dimensionless equivalents of equations (9-10) governing the charge in the electric circuits are respectively,

$$R_c \frac{dq_c}{dt} + \bar{L}_c \frac{d^2 q_c}{dt^2} + \bar{\tau}_{ec} \frac{dw(c)}{dt} = u_c(t), \quad (22)$$

$$\frac{q_p}{\bar{C}_p} + \bar{\tau}_{ep} 2\pi [rw']_a^b = u_p(t). \quad (23)$$

where $\bar{L}_c = L_c/T_c$, $\bar{C}_p = C_p/T_c$ and where $\bar{\tau}_{ec}$ and $\bar{\tau}_{ep}$ are mechanical to electrical coupling coefficients,

$$\bar{\tau}_{ec} = \frac{BIH_0}{R_0^2} \sqrt{\frac{D_0}{\mu_0}}, \quad (24)$$

$$\bar{\tau}_{ep} = \frac{Z_p e_{31} H_0}{C_p}. \quad (25)$$

These coefficients have the dimension of Volts.

2.3 Discretization of the plate's equations

Let us now consider that the eigenfrequencies ω_n and eigenmodes $\phi_n(r, t)$ of the unforced plate without voice coil are known functions. These are the eigenmodes of equation (12) with $p(r, t) = 0$, $\bar{M}_c = 0$ and with boundary conditions (5). They are considered to be known in the present derivation an their exact calculation is presented in appendix A. They are used to perform a modal expansion of the problem. The displacement is hence expressed as a truncated sum of modal contributions,

$$w(r, t) \simeq \sum_{n=1}^N q_{wn}(t) \phi_n(r). \quad (26)$$

with Matlab for the results presented in this article. Let us consider first the loudspeaker's impedance, which is a transfer function commonly measured on loudspeakers. Practically, it can be achieved by forcing the voice coil with a voltage in the form of a harmonic signal at different frequencies and measuring the intensity. Numerically, this is done by considering a forcing vector \vec{u}_0 in the form of a vector full of zeros, except at the position corresponding to u_{0c} . One next compute the response vector with equation (38). The voice coil impedance then reads,

$$Z_c = \frac{i_c(\omega)e^{i\omega t}}{u_{0c}e^{i\omega t}} = \frac{i\omega q_{0c}(\omega)}{u_{0c}}. \quad (39)$$

Another transfer function that will be considered in the following is the transfer function between the displacement at a given position r and the voice coil voltage. After using equation (26) to express the displacement as function of the modal variables, the transfer function we are looking for reads,

$$\frac{w(r, \omega)}{u_{0c}} = \frac{1}{u_{0c}} \sum_{n=1}^N q_{0n}(\omega) \phi_n(r). \quad (40)$$

Similarly, the transfer function between tension at coil and acceleration reads,

$$\frac{a_{r0}(\omega)}{u_c} = -\omega^2 \sum_{n=1}^N q_{0n}(\omega) \phi_n(r_0). \quad (41)$$

Let us consider now the pressure radiated by the plate at a distance L from the plate, on the Z axis. This pressure can be computed using the Rayleigh integral [33],

$$P(L) = -\frac{\Omega^2 \rho}{2\pi} \iint_S \frac{e^{-iKL'}}{L'} W(R) R dR d\theta, \quad (42)$$

where $L' = \sqrt{L^2 + R^2}$ is the distance between the point of interest and a point on the plate and K is the wavenumber,

$$K = \frac{\Omega}{c_0}. \quad (43)$$

In the above equation, the use of capitals letters indicates that dimensional quantities are used. The point is considered to be at a distance greater than the typical size of the plate, $L' \sim L$, and can be put outside of the integral. After a straightforward calculation, the pressure takes then the following form,

$$P(L) = -\frac{\rho H_0 R_0^2}{2\pi T_c^2} \frac{e^{-iKL}}{L} \omega^2 \sum_n q_{0n}(\omega) \chi_{vn}. \quad (44)$$

3 Optimization of the position of the voice coil and the piezoelectric patches

The objective of this section is to address the design of a flat plate excited by a voice coil that approaches the behavior of a classical piston-like loudspeaker. In the low frequency approximation, the latter is viewed as a single mode oscillator coupled to an electrical circuit through electromechanical coupling. The typical transfer functions of such ideal loudspeaker can be obtained by only considering the first plate mode in the model of the previous section, so that $N = 1$ in equation (26). It is plotted in Figure 3a-d and compared to the same voice coil when five modes are retained in the model. In these figures, arbitrary but representative values of the parameters have been chosen. It appears then in Figure 3d that without any particular care taken in the design of this flat loudspeaker, the level of the pressure radiated is not homogeneous, resulting in a poorly equilibrated loudspeaker at frequencies above the second eigenfrequency. Hence, the effective useful bandwidth of this loudspeaker is a narrow range of frequencies above its first eigenfrequency. Conversely, the case $N = 1$ has an increased bandwidth that is more similar to that of a piston-like loudspeaker.

It is envisaged to approach the $N = 1$ behavior by cancelling the effect of resonances of modes 2 and 3 by a careful design of two actuators: one voice coil and one pair of piezoelectric patches. In this optimization process, modes 2 and 3 are addressed differently. Indeed the parameters of the system are adjusted so that the projection of the pressure exerted by the voice coil and the piezoelectric patch on mode 3 equals zero, while mode 2 is cancelled by using appropriate respective values of the amplitudes of the voice coil and piezoelectric voltages u_c , u_{p1} and u_{p2} . In order to ensure a good efficiency of the forcing exerted on mode 2 by the piezoelectric patch, a high value of the piezoelectric modal force of mode 2 is looked for. Finally, in a more compact formal form the optimization procedure can be expressed as:

$$\text{Maximize } \chi_{p2} \text{ with } \chi_{c3} \equiv 0 \text{ and } \chi_{p3} \equiv 0. \quad (45)$$

Equation (33) indicates that $\vec{\chi}_c$ and $\vec{\chi}_p$ depend only on a , b , c and the mode shapes ϕ_n . The latter depend on v_0 , v_p , v_g , \bar{D}_p , $\bar{\mu}_p$, \bar{D}_g , $\bar{\mu}_g$, a , b and c . Consequently, if the material parameters are fixed quantities (see table 1), only the geometric quantities a , b and c are variables for the optimization process. Hence, before performing the optimization procedure, mechanical parameters used for the plate and the piezoelectric actuators have to be known quantities.

The chosen material for the plate is a polymethacrylimide thermoformed foam. This material is used in some modern commercial loudspeakers and its parameters have been estimated by measuring the first two eigenfrequencies of cantilevered plates coming from the same material sample as the one used for the final prototype. The retained material parameters are those ensuring the best fit between experimental frequencies and frequencies predicted by simple finite element computations for different plate sizes. The piezoelectric patches are thin films of PVDF (polyvinylidene

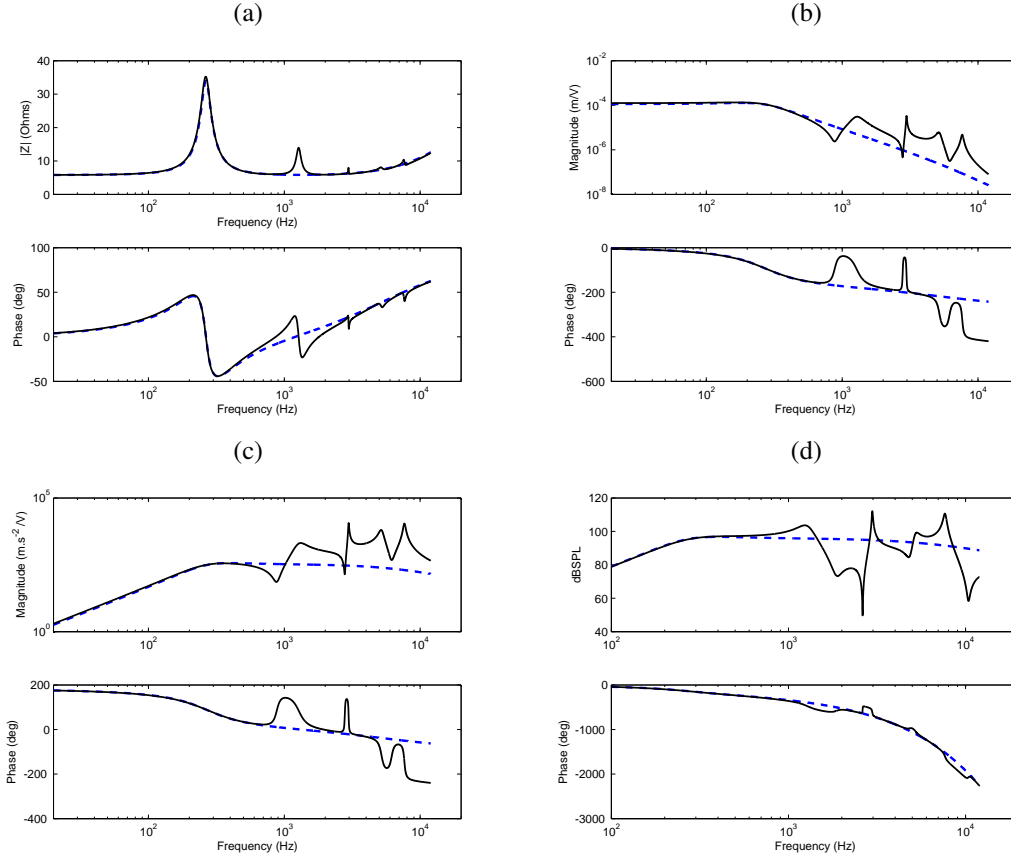


Fig. 3. Typical transfer functions of a clamped flat plate used as a loudspeaker obtained using the present model without considering piezoelectric patches. In blue, $N = 1$ so that its behavior is similar as a single mode piston-like loudspeaker. In black, $N = 5$. (a), voice coil impedance; (b) transfer function between tension at the voice coil outlets and displacement at the center of the plate; (c) transfer function between tension at the voice coil outlets and acceleration at the center of the plate; (d) pressure at 1 meter for a voltage of 2.8V at the voice coil outlets, computed using rayleigh integral calculation.

fluoride) furnished by Piezotech with a complete dataset of the material parameters. In the prototype that is built after this optimization procedure, the piezoelectric patches are glued on the plate using double face adhesive tape. As the mechanical properties of the adhesive were not known, it was decided to arbitrarily set the Young's modulus and the Poisson coefficient equal to that of the piezoelectric material. The density of the adhesive layer was measured with a precision balance and the thickness estimated by measuring the total thickness of a small part of the two-layer laminate with a Keyence precision laser sensor and removing the thickness of the piezoelectric layer. All the material parameters used in this optimization procedure are finally given in Table 1. The voice coil mass may also have a strong influence in the optimisation process. To obtain an estimate of this parameter the radius of the voice coil has been estimated at 1.5 cm so that it coincides with a zero of the third eigenmode of the plate without piezoelectric layer. Such a voice coil was weighted to $M_c = 9.3\text{g}$. This mass is fixed in the optimization process that is now presented.

An optimal loudspeaker satisfying criteria (45) is now sought for in the (a, b, c) space. For each triplet of these parameters, the linear problem detailed in appendix A is solved

Parameter	Rohacell	Piezo	Adhesive
Yng's mod. (MPa)	$E_0 = 220$	$E_p = 1780$	$E_g = 1780$
Poisson's ratio	$\nu_0 = 0.1$	$\nu_p = 0.2$	$\nu_g = 0.2$
Thickness (mm)	$h_0 = 3$	$h_p = 0.04$	$h_g = 0.05$
Density (kg/m^3)	$\rho_0 = 96$	$\rho_p = 1850$	$\rho_g = 500$
Radius (m)	$R_0 = 0.08$		
Piezo coeff. (C/m^2)		$e_{31} = 0.02$	

Table 1. Table of materials properties

to compute the eigenmodes and the projections χ_{p2} , χ_{p3} and χ_{c3} . In Figure 4, the contour levels of χ_{p2} are plotted in the (a, b) plane for different values of c . The contour lines where χ_{p3} and χ_{c3} equal zero are plotted on the same figures in blue and red respectively. Each crossing of the blue and red lines corresponds to a situation where both χ_{p3} and χ_{c3} vanish. Such points are looked for in the vicinity of a maximum of χ_{p2} . It appears that multiple choices of the triplet (a, b, c) are possible. They occur at different points in the (a, b) plane in

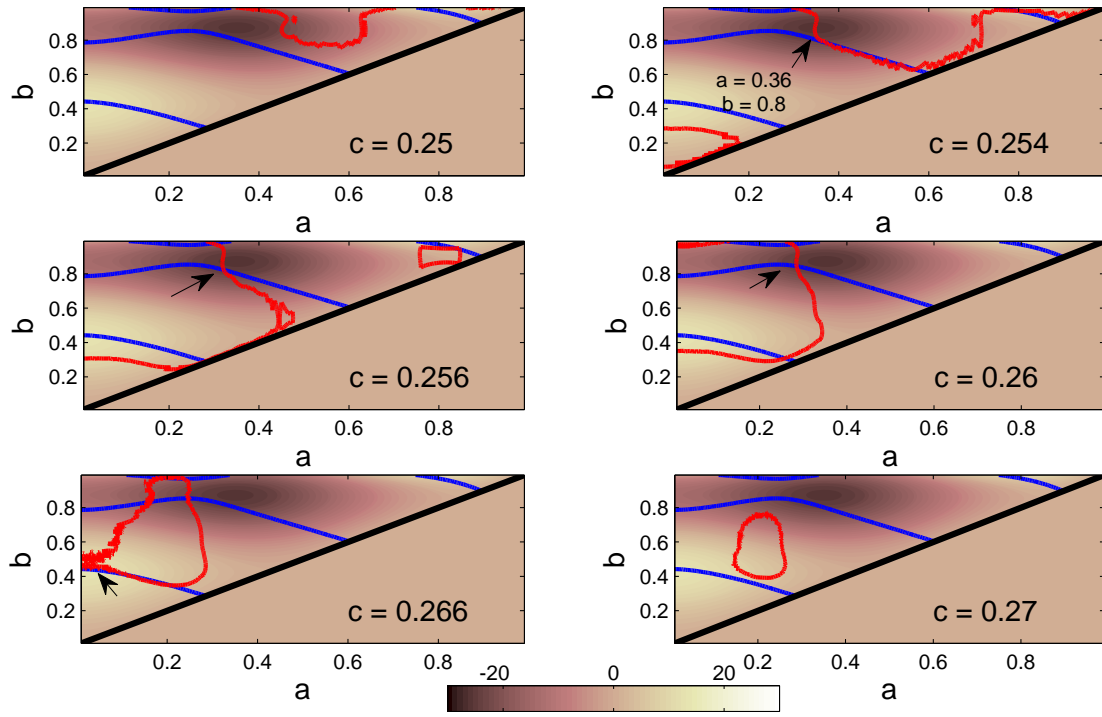


Fig. 4. Contour levels of χ_{p2} in the map (a, b) , zeros of χ_{p3} (blue) and zeros of χ_{c3} (red). Points satisfying the criteria of equation (45) are indicated by an arrow.

the range $c \in [0.254, 0.266]$. Good candidates are indicated by an arrow on these figures. The chosen design is finally the one emphasized at $c = 0.254$ on Figure 4 and the final triplet of chosen parameters is

$$a = 0.36, \quad b = 0.8, \quad c = 0.254. \quad (46)$$

4 Experiments

Based on the design rules obtained in the previous section, the flat plate loudspeaker presented in Figure 5 has been built. Due to practical problems in cutting and gluing manually the piezoelectric patches, the desired radii could not be selected with precision. The following dimensional values of the three geometrical parameters were finally obtained,

$$A = 0.029 \text{ m}, \quad B = 0.063 \text{ m}, \quad C = 0.0195 \text{ m}, \quad (47)$$

the corresponding non-dimensional parameters being,

$$a = 0.363, \quad b = 0.787, \quad c = 0.244. \quad (48)$$

As these parameters are different than that required by the optimization procedure, the criteria (45) is not perfectly satisfied by the prototype. In particular, χ_{c3} and $\chi_{p3} \neq 0$ and mode 3 remains excited. It is expected that this could be improved by more precise and robust manufacturing. Generally

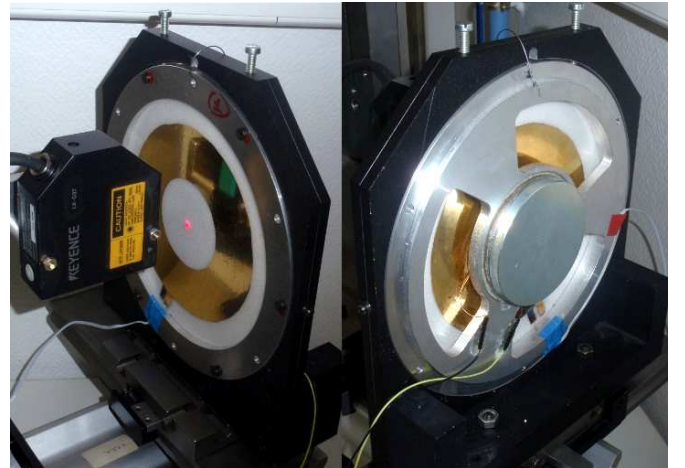


Fig. 5. Photographs of the prototype.

speaking, the standard manufacturing tolerance of piezoelectric material is around 0.2 mm and usually less. Given the geometrical parameters in the experiment, one can expect a precision of the order of 10^{-3} on the geometrical parameters a and b , while it is of 10^{-2} for the present manual procedure.

Mechanical transfer functions predicted by the model are now compared to measurements on the prototype. In the experiments, a National Instrument DAQ card and Labview are used to manage swept sine measurements. Output voltages are sent to the voice coil with a QSC 5050 amplifier and to the piezoelectric patches with a TREK PZD-350 amplifier.

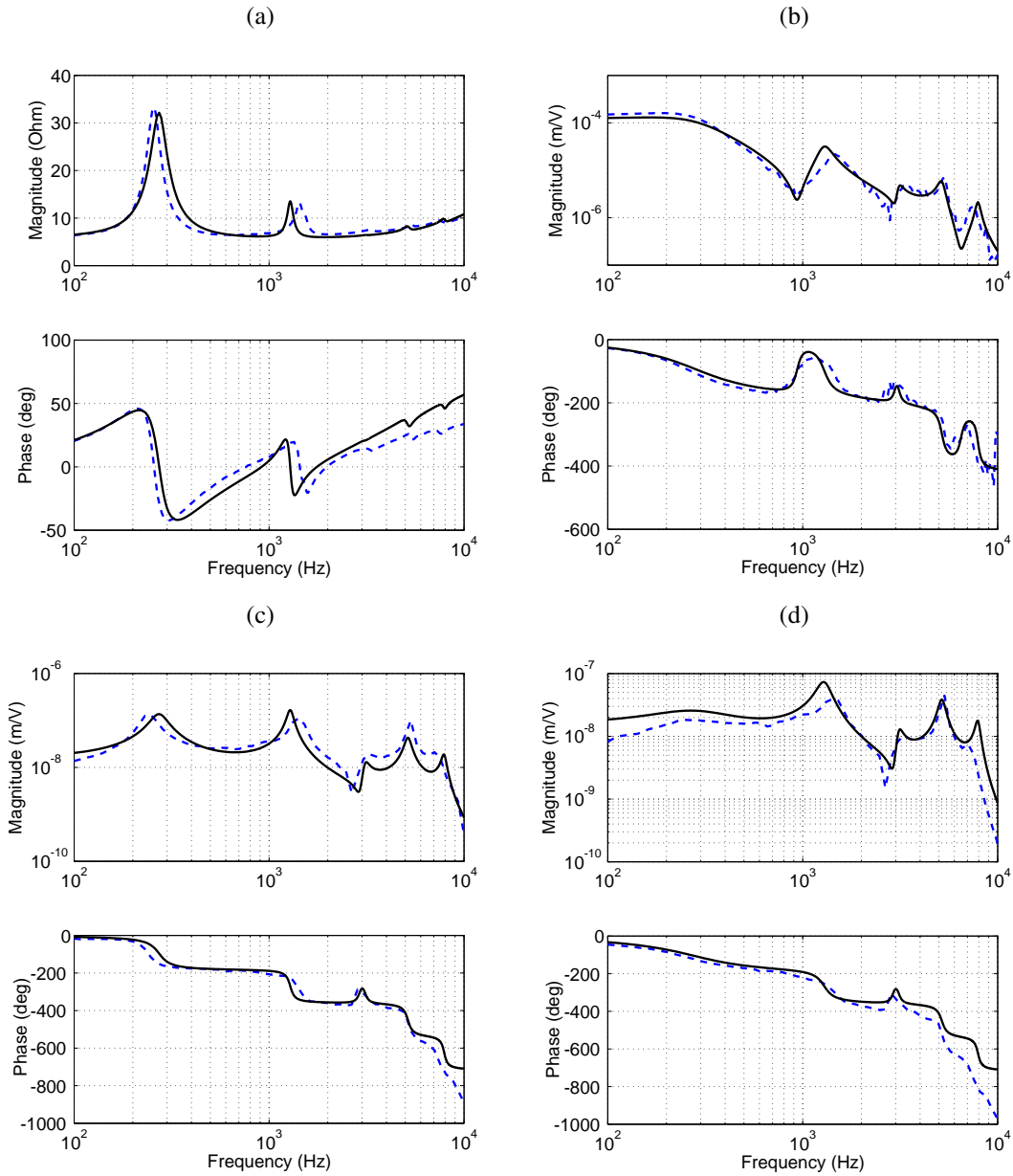


Fig. 6. Comparison of experimental (dashed blue line) and theoretical (plain black line) transfer functions; (a), voice coil impedance; (b), transfer function between voltage at the voice coil outlets and displacement at the center of the plate; (c) transfer function between voltage at the piezoelectric patches outlets and displacement at the center of the plate when the voice coil outlets are not connected; (d), transfer function between voltage at the piezoelectric patches outlets and displacement at the center of the plate when the voice coil outlets are short-circuited.

The displacement of the plate is measured at the center using a Keyence LK-G37 laser displacement. Four different resulting transfer functions are plotted on Figure 6 and compared to the theory:

- (a) the voice coil impedance,
- (b) the transfer function between voltage at the voice coil inlets and displacement at the center of the plate (w_{r_0}/u_c),
- (c) the transfer function between tension at the piezoelectric patches outlets and displacement at the center of the plate when the voice coil outlets are not connected (w_{r_0}/u_c with $\bar{\tau}_c$ forced to 0)
- (d) the same as the latter when the voice coil outlets are

short-circuited (w_{r_0}/u_c).

The modal dampings of modes 1 and 2 have been adjusted so that the height of the peaks are the same for theory and experiments on the impedance curves of Figure 6(a). Precision of the identification of damping using impedance peaks was insufficient for higher modes, it was hence chosen to adjust modal damping of these modes so that we observe the best fit between theory and experiments in the transfer function of Figure 6(b). Finally, the five diagonal coefficients of the matrix C of equation (35) are set to [2.4, 3.6, 7, 15, 17]. It has to be noted that eigenmodes of the system are independent of the diagonal terms in the damping matrix because

these terms do not introduce coupling between modes in the mechanical system (35). Consequently, results of the the optimization procedure presented in section 3 are not affected by the adjustment of these damping coefficients.

The first observation that can be made from the the experimental and theoretical curves of Figure 6 is that a good agreement exists between experiments and a model where only the damping has been adjusted. Indeed, it has to be recalled that all other parameters have been identified using distinct experiments: dynamic tests on beams for the plate's material, manufacturer data for the piezoelectric material, electrical measurements for the static resistance and impedance of the voice-coil, weightings for the different masses. Only the Young's modulus of the glue has been arbitrarily chosen. However, this parameter was adjusted in order to improve the agreement. Slight improvements of the model's results have been observed when E_g is strongly increased, but changes were not significant enough to justify a change in the value selected in the previous section. It has to be noted that in the case presented here, contrary to the objectives of the optimization performed in section 3, mode 3 remains excited by both the piezoelectric patches and the voice coil. This is clearly visible on each of the plots. This may be due to the imprecisions occurring during the manufacturing process.

Let us now address the cases where both the voice coil and the piezoelectric patches are used to force the plate. It is desired to approach a case where only the first mode is excited, so that we obtain a better spectral equilibrium of the radiated power. On Figures 7 and 8, the transfer function between voltage at the voice coil and the displacement at the center of the plate is plotted in five different cases:

- . Only the voice coil is used (piezoelectric patches short circuited), theoretically and experimentally. This case is in practice the same as in Figure 6b
- . The same electrical signal is sent to the piezoelectric patches, but with an amplitude multiplied by 250, theoretically and experimentally.
- . A virtual case where only the first mode is excited by the voice coil ($N = 1$ theoretical approximation).

The chosen factor 250 is the one that displays the best fit between the $N = 1$ approximation and the experimental result. On these plots we observe that it is possible to reduce significantly the amplitude of anti-resonance and resonance associated to mode 2 on both displacement and acceleration plots. However, due to the fact that χ_{p3} and χ_{e3} do not vanish, mode 3 remains excited.

Finally, the experimental and theoretical radiated power on the axis at 84 cm expressed in dB_{SPL} units is plotted on Figure 9a and Figure 9b in two different cases. In the first case, a white noise signal of 0.48V rms amplitude is sent to the voice coil while the piezoelectric patches are shunted ($u_{p1,2} = 0$). This case is referred to as the non-controlled system. In the second case, the same signal amplified 250 times is sent to the piezoelectric patches (120V rms). This case is referred to as the controlled system. Experimentally, the loudspeaker is baffled in a wood plane of 60×65 cm and

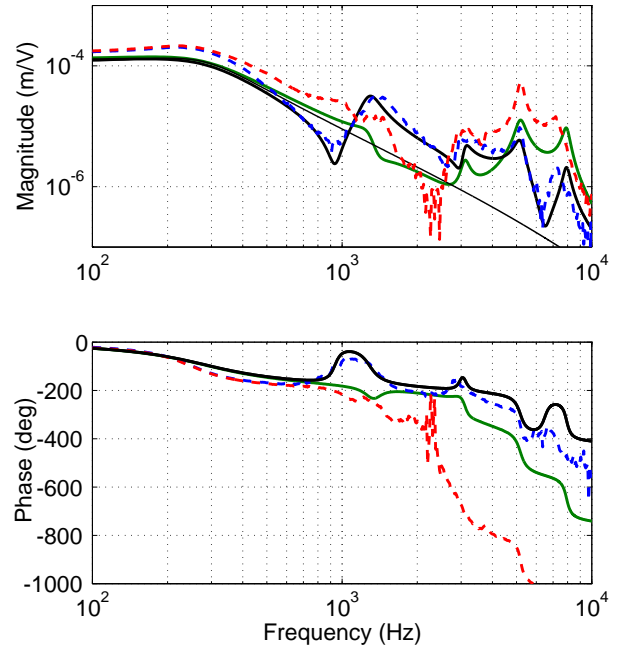


Fig. 7. Transfer function between voice coil voltage and displacement at the center of the plate, comparison of non controlled system (theory in black plain line, experiment in blue dashed line) and controlled system (theory in green plain line, experiment in red dashed line). The theoretical case $N = 1$ is plotted on the same figure with a thin black line to serve as a guide for the eyes representing the ideal case.

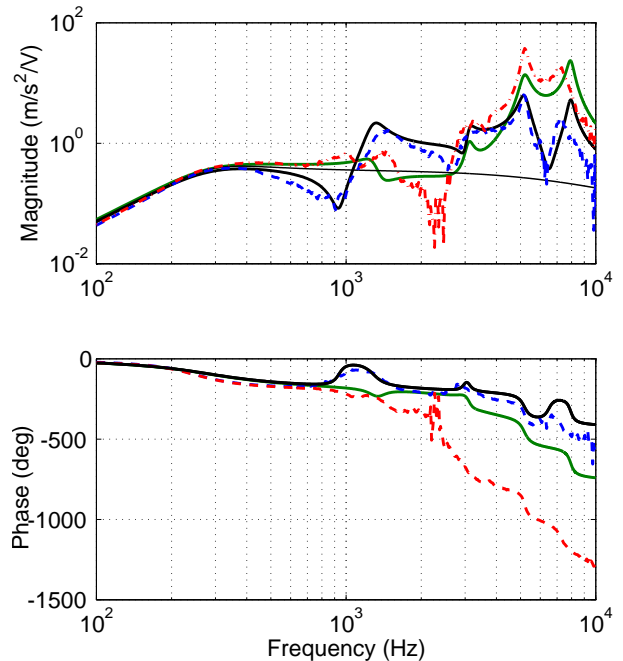


Fig. 8. Transfer function between voice coil voltage and acceleration at the center of the plate, comparison of non controlled and controlled systems. Legends are the same as Figure 7.

measurements are performed in an anechoic chamber. It is known that for acoustical wavelengths equal or greater than the typical size of the plate, the rearward radiation interferes with the frontward direct radiation [33], so that the results can not be compared with Rayleigh integral computations, which corresponds to an infinite baffle. Above this grayed range, experiments and theory are in good agreement.

The radiation of the uncontrolled system presents a peak at 1500Hz, followed by a strong hole due the resonance and antiresonance of the second mode. The antiresonance is strongly reduced in the controlled system. A succession of resonance and antiresonance is also observed for the third mode around 3000 Hz. The controlled system presents also a reduced antiresonance. Finally, if we tolerate a maximum difference of 10dB in the pressure radiated by the plate, we can conclude that the system is able to extend the useful bandwidth from [200Hz,1500Hz] up to [200Hz,4000Hz].

5 Conclusion

In order to reduce the depth of the devices used to reproduce sound, one can envisage to use a clamped flat plate as a loudspeaker. In this article, the dynamics of a clamped plate excited by a voice coil at a given radius has been modeled. In order to circumvent the problems due to the vibrations of the plate along undesirable modes, we investigated the use of an additional forcing exerted by annular piezoelectric patches. An optimization has been performed to design a system where the modal force due to the voice coil and the piezoelectric patches second and third modes is minimized. A prototype has then been presented and transfer functions measured and predicted by the model have been successfully compared. Next, control tests have been presented, showing encouraging results. Indeed the radiated power shows that forcing the system with both the voice coil and the piezoelectric patches at appropriate respective amplitudes, the effects of the antiresonance and resonance of the second mode are less pronounced. Concerning the third mode, the objective was to design actuators which geometries allowed to cancel the forcing on this particular mode. The manufacturing as not precise enough to fully satisfy this objective.

Improvements to this study are multiple. Firstly, some work should be made to improve the precision of the manufacturing of the piezoelectric patches. Better understanding of the glue mechanical properties could also induce better agreement between theoretical and experimental results and thus improve the optimization process. Different plates could also be envisaged. Indeed, the thermoformed foam was used because it is commonly used in conical loudspeakers. This does not mean that it is the best material for the present application. Guidelines for the choice of this material could be found for instance in studies that look for parameters that maximize the piezoelectric coupling on sandwich beams [34]. Multiple pairs of piezoelectric patches or supplementary voice coils could also be envisaged to extend the bandwidth of the plate. Piezoelectric materials of different shapes or with spatially varying polarization could also be considered to design so-called modal actuators that could

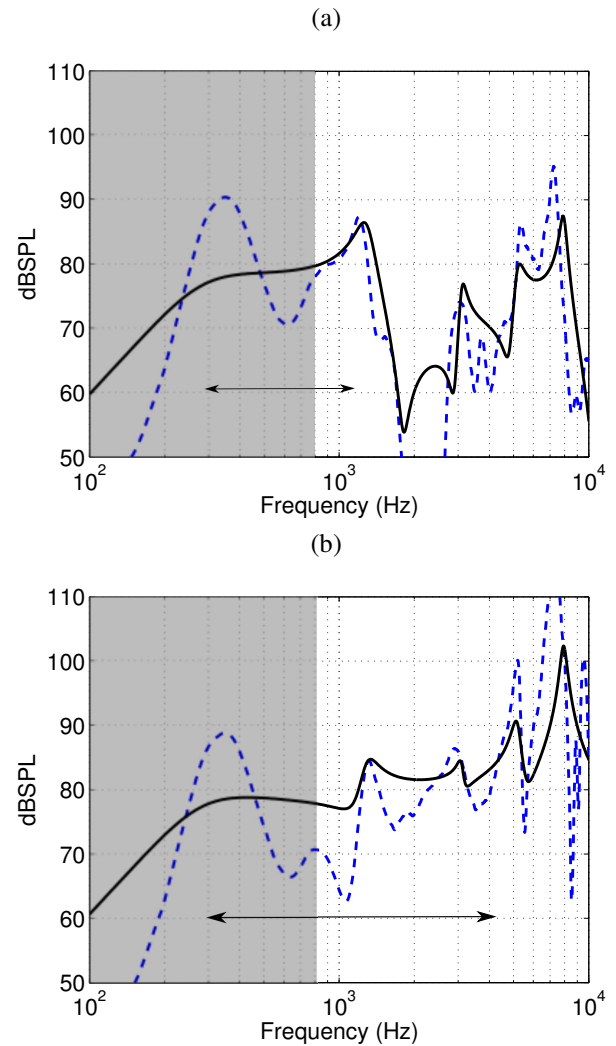


Fig. 9. Power radiated by the plate on axis at 84 cm, comparison of non controlled and controlled systems. Experiments in dashed blue and theory in plain black. Grayed region indicates the frequency range where backward radiation interferes with frontward radiation, which is not taken into account by the model. The arrow indicates the bandwidth of the loudspeaker where a maximum 10 dB difference between minimum and maximum value is tolerated. (a), uncontrolled system; (b) controlled system.

improve mode selectivity [32, 35]. Finally, nonlinear aspects have been overlooked in this work and should be included in the model to address the distortions that arise at high vibration amplitudes [36].

Acknowledgements

The authors would like to thank Cyrille Dodard, from Cabasse, for the fruitful interactions and the building of the loudspeaker prototype.

Appendix A: Eigenmodes and eigenfrequencies of the unforced plate without voice coil

The plate equation (4) is rewritten in the form of a union of homogeneous problems,

$$\begin{aligned} D_0 \Delta^2 W(R, T) + \mu_0 \ddot{W}(R, T) &= 0 \text{ in } \Omega_1 \text{ and } \Omega_3, \\ (D_0 + D_p) \Delta^2 W(R, T) + (\mu_0 + \mu_p) \ddot{W}(R, T) &= 0 \text{ in } \Omega_2, \end{aligned} \quad (49)$$

where $\Omega_1 \equiv R \in [0, A]$, $\Omega_2 \equiv R \in [A, B]$ and $\Omega_3 \equiv R \in [B, R_0]$. To the set of local equations (4), a set of boundary conditions has to be added. These boundary conditions are the continuity of the displacement W , the rotation $\partial W / \partial R$ the momentum and the shear at $R = A$ and $R = B$ and the boundary conditions of a plate clamped at $R = R_0$,

$$\begin{aligned} [W]_{A^-}^{A^+} &= 0, [\partial W / \partial R]_{A^-}^{A^+} = 0, [Q]_{A^-}^{A^+} = 0, [\mathcal{M}]_{A^-}^{A^+} = 0, \\ [W]_{B^-}^{B^+} &= 0, [\partial W / \partial R]_{B^-}^{B^+} = 0, [Q]_{B^-}^{B^+} = 0, [\mathcal{M}]_{B^-}^{B^+} = 0, \quad (50) \\ W(R_0) &= 0, \frac{\partial W}{\partial R}(R_0) = 0. \end{aligned}$$

In the particular case of a displacement independent of the polar angle, the momentum reads:

$$\begin{aligned} \mathcal{M} &= -D_0 \frac{\partial^2 W}{\partial R^2} - D_0 \nu_0 \frac{1}{R} \frac{\partial W}{\partial R} \quad \text{in } \Omega_1 \text{ and } \Omega_3 \\ \mathcal{M} &= -(D_0 + D_p) \frac{\partial^2 W}{\partial R^2} - (D_0 \nu_0 + D_p \nu_p) \frac{1}{R} \frac{\partial W}{\partial R} \quad \text{in } \Omega_2, \end{aligned} \quad (51)$$

and the shear has the following expression:

$$\begin{aligned} Q &= -D_0 \frac{\partial}{\partial R} \Delta W \quad \text{in } \Omega_1 \text{ and } \Omega_3 \\ Q &= -(D_0 + D_p) \frac{\partial}{\partial R} \Delta W \quad \text{in } \Omega_2. \end{aligned} \quad (52)$$

Introducing the non-dimensional radius, displacement, time and force given in equation (11) the non-dimensional local equilibrium equation (49) becomes,

$$\begin{aligned} \Delta^2 w + \ddot{w} &= 0 \quad \text{in } \Omega_1 \text{ and } \Omega_3, \\ \bar{D}_p \Delta^2 w + \bar{\mu}_p \ddot{w} &= 0 \quad \text{in } \Omega_2. \end{aligned} \quad (53)$$

In non-dimensional form, the boundary conditions have then

the following expanded form,

$$[w]_{a^-}^{a^+} = 0, \quad (54)$$

$$[\partial w / \partial r]_{a^-}^{a^+} = 0, \quad (55)$$

$$\left. \frac{\partial}{\partial r} \Delta w \right|_{a^-} - (1 + \bar{D}_p) \left. \frac{\partial}{\partial r} \Delta w \right|_{a^+} = 0, \quad (56)$$

$$\begin{aligned} \left. \frac{\partial^2 w}{\partial r^2} + \nu_0 \frac{1}{r} \frac{\partial w}{\partial r} \right|_{a^-} \\ - (1 + \bar{D}_p) \left. \frac{\partial^2 w}{\partial r^2} + (\nu_0 + \bar{D}_p \nu_p) \frac{1}{r} \frac{\partial w}{\partial r} \right|_{a^+} = 0, \end{aligned} \quad (57)$$

$$[w]_{b^-}^{b^+} = 0, \quad (58)$$

$$[\partial w / \partial r]_{b^-}^{b^+} = 0, \quad (59)$$

$$\left. \frac{\partial}{\partial r} \Delta w \right|_{b^+} - (1 + \bar{D}_p) \left. \frac{\partial}{\partial r} \Delta w \right|_{b^-} = 0, \quad (60)$$

$$\begin{aligned} \left. \frac{\partial^2 w}{\partial r^2} + \nu_0 \frac{1}{r} \frac{\partial w}{\partial r} \right|_{b^+} \\ - (1 + \bar{D}_p) \left. \frac{\partial^2 w}{\partial r^2} + (\nu_0 + \bar{D}_p \nu_p) \frac{1}{r} \frac{\partial w}{\partial r} \right|_{b^-} = 0, \end{aligned} \quad (61)$$

$$w(1) = 0, \quad (62)$$

$$\frac{\partial w}{\partial r}(1) = 0. \quad (63)$$

The eigenfrequencies and eigenmodes of equation (53) with boundary conditions (54-63) are now sought for. It is practically done by introducing a solution of the form

$$w(r, t) = \varphi(r) e^{i\omega t} \quad (64)$$

in equation (53). The latter now reads,

$$\begin{aligned} \Delta^2 w - \lambda^4 w &= 0 \quad \text{in } \Omega_1 \text{ and } \Omega_3 \\ \Delta^2 w - \alpha^4 \lambda^4 w &= 0 \quad \text{in } \Omega_2, \end{aligned} \quad (65)$$

where

$$\lambda^4 = \omega^2 \quad (66)$$

and

$$\alpha^4 = \frac{1 + \bar{\mu}_p}{1 + \bar{D}_p}. \quad (67)$$

The solutions of these well known ordinary differential equa-

tions are combinations of Bessel functions,

$$\varphi_1(r) = A_1 J_0(\lambda r) + A_2 I_0(\lambda r), \quad \text{in } \Omega_1 \quad (68)$$

$$\varphi_2(r) = A_3 J_0(\alpha \lambda r) + A_4 Y_0(\alpha \lambda r) + A_5 I_0(\alpha \lambda r) + A_6 K_0(\alpha \lambda r), \quad \text{in } \Omega_2 \quad (69)$$

$$\varphi_3(r) = A_7 J_0(\lambda r) + A_8 Y_0(\lambda r) + A_9 I_0(\lambda r) + A_{10} K_0(\lambda r), \quad \text{in } \Omega_3 \quad (70)$$

Introducing these solutions in the boundary conditions expressions leads to a linear problem,

$$M_A \vec{A} = 0, \quad (71)$$

where \vec{A} is a column vector with 10 elements corresponding to the amplitudes A_n , $n \in [1, 10]$ and M_A is the matrix which coefficients are deduced from the boundary conditions expressions. A non trivial solution exists if

$$\det(M_A) = 0. \quad (72)$$

The numerical resolution of this last equation gives the discrete values of λ_n , which then gives the eigenfrequencies using equation (66). Introducing a particular value λ_n in the linear problem (71) gives the associated eigenmode through the vector \vec{A}_n . The associated eigenmode $\phi_n(r)$ is the union of functions $\varphi_{1...3}$ in their respective domains. One has then to choose a convention for the norm of the eigenmodes. Let us define a scalar product in the domain Ω :

$$\langle f, g \rangle = \int_S f g dS = 2\pi \int_0^1 f g r dr. \quad (73)$$

The chosen convention for the normalization is,

$$\langle \bar{\mu}(r) \phi_n(r), \phi_n(r) \rangle = 1, \quad (74)$$

where $\bar{\mu}$ describe the distribution of surface density of the plate, and reads,

$$\bar{\mu}(r) = 1 + [H(r-a) - H(r-b)] \bar{\mu}_p. \quad (75)$$

By definition, the eigenmodes are orthogonal with respect to the mass and rigidity operators,

$$\langle \bar{\mu}(r) \phi_n(r), \phi_m(r) \rangle = \delta_{nm}, \quad (76)$$

$$\langle \bar{D}(r) \phi_n(r), \phi_m(r) \rangle = \omega_m^2 \delta_{nm}, \quad (77)$$

where \bar{D} describe the distribution of rigidity of the plate,

$$\bar{D}(r) = 1 + [H(r-a) - H(r-b)] \bar{D}_p, \quad (78)$$

and δ is the Kronecker symbol. The eigenmodes defined here serve as a basis for the full problem defined in section 2.



Fig. 10. Schematic view of the five layers problem.

Appendix B: Five layers problem: equivalent three layers problems

Provided that the Young's modulus of the glue is of the same order as the other materials, the assumption that the deformation varies linearly with Z is still valid. We have to solve a problem of a five layer plate, as sketched in Figure 10. The momentum has now the following expression in Cartesian coordinates [37],

$$\begin{aligned} \mathcal{M} &= \int_{-h_0/2-h_g-h_p}^{h_0/2+h_g+h_p} \sigma_{XX} Z dZ \quad (79) \\ &= -(D_0 + D_g + D'_p) \frac{\partial^2 W}{\partial X^2} - (v_0 D_0 + v_g D_g + v_p D'_p) \frac{\partial^2 W}{\partial Y^2}, \quad (80) \end{aligned}$$

with,

$$D_g = \frac{E_g}{1 - \nu_g^2} \left(\frac{H_g H_0^2}{2} + H_g^2 H_0 + \frac{2H_g^3}{3} \right) \quad (81)$$

$$D'_p = \frac{E_p}{1 - \nu_p^2} \left(\frac{H_p (H_0 + H_g)^2}{2} + H_p^2 (H_0 + H_g) + \frac{2H_p^3}{3} \right) \quad (82)$$

The prime is used to avoid confusion with D_p defined in the three layer problem [30]. The momentum then takes the following form in cylindrical coordinates [37],

$$\mathcal{M} = -(D_0 + D_g + D'_p) \frac{\partial^2 W}{\partial R^2} - (v_0 D_0 + v_g D_g + v_p D'_p) \frac{1}{R} \frac{\partial W}{\partial R}. \quad (83)$$

In non dimensional form, the continuity equation for the momentum has the following expression at $r = a$,

$$\begin{aligned} \frac{\partial^2 w}{\partial r^2} + v_0 \frac{1}{r} \frac{\partial w}{\partial r} \Big|_{a^-} - (1 + \bar{D}'_p + \bar{D}_g) \frac{\partial^2 w}{\partial r^2} \\ + (v_0 + \bar{D}'_p v_p + \bar{D}_g v_g) \frac{1}{r} \frac{\partial w}{\partial r} \Big|_{a^+} = 0. \quad (84) \end{aligned}$$

This last expression can be rewritten in the following form,

$$\begin{aligned} \frac{\partial^2 w}{\partial r^2} + v_0 \frac{1}{r} \frac{\partial w}{\partial r} \Big|_{a^-} - (1 + \bar{D}_{pg}) \frac{\partial^2 w}{\partial r^2} \\ + (v_0 + \bar{D}_{pg} v_{pg}) \frac{1}{r} \frac{\partial w}{\partial r} \Big|_{a^+} = 0, \quad (85) \end{aligned}$$

with,

$$\bar{D}_{pg} = \bar{D}'_p + \bar{D}_g \quad (86)$$

$$v_{pg} = \frac{\bar{D}'_p v_p + \bar{D}_g v_g}{\bar{D}'_p + \bar{D}_g} \quad (87)$$

Hence, the five layer problem can be modeled using the same equations as presented in section 2, provided that the following change of parameters is done :

$$\bar{D}_p \longrightarrow \bar{D}_{pg} \quad (88)$$

$$v_p \longrightarrow v_{pg} \quad (89)$$

$$\bar{\mu}_p \longrightarrow \bar{\mu}_{pg} = \bar{\mu}_p + \bar{\mu}_g \quad (90)$$

$$Z_p \longrightarrow Z_{pg} = \frac{H_0 + H_p + H_g}{2} \quad (91)$$

References

- [1] Thiele, N., 1971. "Loudspeakers In Vented Boxes: Part 1". *Journal Of The Audio Engineering Society*, **19**, pp. 181–191.
- [2] Thiele, N., 1971. "Loudspeakers in Vented Boxes: Part 2". *Journal Of The Audio Engineering Society*, **19**(6), pp. 471–483.
- [3] Small, R. H., 1972. "Closed-Box Loudspeaker Systems-Part 1: Analysis". *Journal Of The Audio Engineering Society*, **20**(10), pp. 798–808.
- [4] Small, R. H., 1973. "Closed-Box Loudspeaker Systems-Part 2: Synthesis". *Journal Of The Audio Engineering Society*, **21**(1), pp. 11–18.
- [5] Kuo, D., Shiah, Y. C., and Huang, J. H., 2011. "Modal Analysis of a Loudspeaker and Its Associated Acoustic Pressure Field". *Journal of Vibrations and Acoustics-Transactions of the ASME*, **133**(3).
- [6] Bédard, M., and Berry, A., 2008. "Development of a directivity-controlled piezoelectric transducer for sound reproduction". *Journal of Sound and Vibration*, **311**(3–5), pp. 1271–1285.
- [7] Prokofieva, E., Horoshenkov, K. V., and Harris, N., 2002. "Intensity Measurements of the Acoustic Emission from a DML Panel". In *Audio Engineering Society Convention 112*.
- [8] Zhang, S., Shen, Y., Shen, X., and Zhou, J., 2006. "Model Optimization of Distributed-Mode Loudspeaker Using Attached Masses". *Journal Of The Audio Engineering Society*, **54**(4), pp. 295–305.
- [9] Berkhout, A. J., 1993. "Acoustic control by wave field synthesis". *Journal Of The Acoustical Society Of America*, **93**(5), pp. 2764–2778.
- [10] Pueo, B., López, J. J., Escolano, J., and Hörchens, L., 2010. "Multiactuator Panels for Wave Field Synthesis: Evolution and Present Developments". *Journal Of The Audio Engineering Society*, **58**(12), pp. 1045–1063.
- [11] Alper, S., and Magrab, E. B., 1970. "Radiation from forced harmonic vibrations of a clamped circular plate in an acoustic fluid". *Journal Of The Acoustical Society Of America*, **48**, pp. 681–691.
- [12] Preumont, A., 2002. *Vibration Control of Active Structures: An Introduction*, 2nd ed. Kluwer Academic Publishers.
- [13] Lin, Y. H., and Chu, C. L., 1996. "Active flutter control of a cantilever tube conveying fluid using piezoelectric actuators". *Journal of Sound and Vibration*, **196**(1), pp. 97–105.
- [14] Block, J. J., and Strganac, W., 1998. "Applied Active Control for a Nonlinear Aeroelastic Structure". *Journal of Guidance and Control*, **21**(6), pp. 838–845.
- [15] Hagood, N., and von Flotow, A., 1991. "Damping of structural vibrations with piezoelectric materials and passive electrical networks". *Journal of Sound and Vibration*, **146**(2), pp. 243–268.
- [16] Tylikowski, A., 2001. "Control of circular plate vibrations via piezoelectric actuators shunted with a capacitive circuit". *Thin-Walled Structures*, **39**, pp. 83–94.
- [17] Bisegna, P., Caruso, G., and Maceri, F., 2006. "Optimized electric networks for vibration damping of piezoactuated beams". *Journal of Sound and Vibration*, **289**(4-5), pp. 908–937.
- [18] Anton, S. R., and Sodano, H. A., 2007. "A review of power harvesting using piezoelectric materials (2003—2006)". *Smart Materials and Structures*, **16**, pp. 1–21.
- [19] De Marqui Junior, C., Erturk, A., and Inman, D. J., 2009. "An electromechanical finite element model for piezoelectric energy harvester plates". *Journal of Sound and Vibration*, **327**(1-2), pp. 9–25.
- [20] Masana, R., and Daqaq, M. F., 2011. "Electromechanical Modeling and Nonlinear Analysis of Axially Loaded Energy Harvesters". *Journal of Vibration and Acoustics*, **133**(1), p. 011007.
- [21] Doaré, O., and Michelin, S., 2011. "Piezoelectric coupling in energy-harvesting fluttering flexible plates: linear stability analysis and conversion efficiency". *Journal of Fluids and Structures*, **27**(8), pp. 1357–1375.
- [22] Fuller, C. R., Hansen, C. H., and Snyder, S. D., 1991. "Experiments on active control of sound radiation from a panel using a piezoceramic actuator". *Journal of Sound and Vibration*, **150**(2), pp. 179–190.
- [23] Tzou, H., and Zhou, Y., 1995. "Dynamics and control of non-linear circular plates with piezoelectric actuators". *Journal of Sound and Vibration*, **188**(2), pp. 189–207.
- [24] Lee, J. C., and Chen, J. C., 1999. "Active control of sound radiation from rectangular plates using multiple piezoelectric actuators". *Applied Acoustics*, **57**(4), pp. 327–343.
- [25] Chen, K., Chen, G., Pan, H., and Li, S., 2008. "Secondary actuation and error sensing for active acoustic structure". *Journal of Sound and Vibration*, **309**(1-2), pp. 40–51.
- [26] Larbi, W., Deu*, J. F., Ciminello, M., and Ohayon, R., 2010. "Structural-Acoustic Vibration Reduction Using Switched Shunt Piezoelectric Patches: A Finite Element Analysis". *Journal of Vibration and Acoustics-*

Transactions of the ASME, **132**(5), p. 051006.

- [27] Gardonio, P., Bianchi, E., and Elliott, S. J., 2004. “Smart panel with multiple decentralized units for the control of sound transmission. Part I: theoretical predictions”. *Journal of Sound and Vibration*, **274**(1–2), pp. 163–192.
- [28] Gardonio, P., Bianchi, E., and Elliott, S. J., 2004. “Smart panel with multiple decentralized units for the control of sound transmission. Part II: design of the decentralized control units”. *Journal of Sound and Vibration*, **274**(1–2), pp. 193–213.
- [29] Bianchi, E., Gardonio, P., and Elliott, S. J., 2004. “Smart panel with multiple decentralized units for the control of sound transmission. Part III: control system implementation”. *Journal of Sound and Vibration*, **274**(1–2), pp. 215–232.
- [30] Lee, C. K., and Moon, F. C., 1989. “Laminated piezopolymer plates for torsion and bending sensors and actuators”. *Journal Of The Acoustical Society Of America*, **85**, pp. 2432–2439.
- [31] Lee, C. K., 1990. “Theory of laminated piezoelectric plates for the design of distributed sensors actuators .1. Governing equations and reciprocal relationships”. *Journal Of The Acoustical Society Of America*, **87**, pp. 1144–1158.
- [32] Lee, C. K., and Moon, F. C., 1990. “Modal Sensors/Actuators”. *Journal of Applied Mechanics*, **57**(2), pp. 434–441.
- [33] Pierce, A. D., 1989. *Acoustics: An Introduction to Its Physical Principles and Applications*.
- [34] Ducarne, J., Thomas, O., and Deü, J. F., 2012. “Placement and dimension optimization of shunted piezoelectric patches for vibration reduction”. *Journal of Sound and Vibration*, **331**(14), pp. 3286–3303.
- [35] Donoso, A., and Bellido, J. C., 2009. “Distributed piezoelectric modal sensors for circular plates”. *Journal of Sound and Vibration*, **319**(1-2), pp. 50–57.
- [36] Quaegebeur, N., and Chaigne, A., 2008. “Nonlinear vibrations of loudspeaker-like structures”. *Journal of Sound and Vibration*, **309**(1-2), pp. 178–196.
- [37] Mansfield, E. H., 1989. *The Bending and Stretching of Plates*, Second edition ed. Cambridge University Press.